Phospholipid chain interactions drive cholesterol induced liquid-ordered – liquid-disordered phase coexistence in lipid membranes

W.F. Drew Bennett^{1,3}, Joan-Emma Shea¹, and D. Peter Tieleman^{2,3}

¹University of California, Santa Barbara, California 93106, United States

² University of Calgary, Department of Biological Sciences and Centre for Molecular Simulation, 2500 University Drive, Calgary AB, T2N 1N4.

³corresponding authors: tieleman@ucalgary.ca; wfdbennett@gmail.com

Abstract

Cholesterol is a key component of eukaryotic membranes but its role in cellular biology in general and in lipid rafts in particular remains controversial. Model membranes have been extensively used to determine the phase behavior of ternary mixtures of cholesterol, a saturated lipid and an unsaturated lipid – with liquid-ordered and liquid-disordered phase coexistence. Despite many different experiments that determine lipid phase diagrams, we lack an understanding of the molecular level driving forces for liquid phase coexistence in bilayers with cholesterol. Here we use atomistic molecular dynamics computer simulations to address the driving forces for phase coexistence in ternary lipid mixtures. Domain formation is directly observed in a long time scale simulation of a mixture of DSPC, unsaturated DLiPC, and cholesterol. Free energy calculations for the exchange of the saturated and unsaturated lipids between the ordered and disordered phases give insight into the mixing behavior. We show that domain formation is due to large favorable enthalpic interactions of the saturated lipid in the ordered phase, and a large unfavorable entropy for the unsaturated lipid to be in the ordered phase. Martini coarse-grained simulations capture the unfavorable free energy of mixing, but do not reproduce the entropic contribution due to the reduced representation of the phospholipid tails. Phospholipid tails and their degree of unsaturation are key energetic contributors to lipid phase separation.

Introduction

Lipid mixing is a fundamental problem in cellular biology. How lipids self-associate and interact with membrane proteins is crucial for the function of cell membranes. The lipid raft hypothesis was initially conceived to explain the difference in membrane sorting between the apical and basal sides of epithelial cells ¹, although membrane domains had been suggested earlier ². The idea of membrane sorting, with cholesterol-sphingomyelin interactions as an organizing principle, changed the way lipid membranes had been traditional viewed, with a much-enhanced bioactive role. "Lipid raft" has become a broadly used term, but lipids rafts are generally thought to be small (10-100 nm), dynamic domains in cell membranes enriched in cholesterol, sphingomyelin (or other saturated lipids), and specific membrane proteins 3. There has been considerable research and debate on the existence and characterization of rafts because of their implicated role in cellular signaling and signaling related disease ³. Stimulated emission depletion (STED) nanoscopy has been used to observe inhomogeneity in living cells ⁴ and point to the importance of sphingolipids and the cytoskeleton in domain formation ⁵. The composition and nanometer resolution accessible by high-resolution secondary ion mass spectrometry has called into question a central tenant of the current raft hypothesis: locally enriched regions of cholesterol, although sphingomyelin domains have been observed 6-9. It is becoming clear that cells have dynamic nanoscale domains, likely enriched in different lipids and membrane associated proteins depending on organism, cell type, and organelle. We are gaining an appreciation for the complexity and intricacies of cell membranes and their molecular level interactions and the role of lipids in transmembrane protein function is still being characterized.

A major bottleneck to study cellular membranes is their diversity, with thousands of types of lipids, membrane proteins, and active processes such as enzyme catalysis, vesicle fussion and fission, and lipid transport proteins. Eukaryotic membranes display a gradient in the structure and lipid composition from the endoplasmic reticulum to the plasma membrane; from low (0-5 mol%) to high (25-50 mol%) cholesterol content ¹⁰. There is also a high concentration of transmembrane proteins, and interactions with the cytoskeleton, which has been also suggested as a main membrane sorting and clustering 11. Due to the many hurdles for characterizing in vivo lipid domains, model vesicles have been used extensively ¹²⁻¹⁹. It has been observed that cholesterol induces phase separation in model giant unilamellar vesicle (GUV) mixtures with saturated and unsaturated lipids 20, with a liquid-ordered (l₀) phase coexistence with a liquid-disordered (l_d) phase. Great effort has been made in characterizing the phase diagrams for cholesterol containing lipid bilayers and monolayers ²¹. Ternary and quaternary phase diagrams have been determined for many lipids with cholesterol, using NMR, fluorescence spectroscopy, and many other methods ^{22–26}. STED nanoscopy recently showed that many fluorescently labeled lipid analogs mis-partition between lo and ld domains in GUVs compared to their native

counterparts and importantly GUVs composed of DOPC/SM/Cholesterol are probably not good models for cell membranes ²⁷.

The fundamental basis for membrane domains is lipid-lipid and lipid-protein interactions, which are difficult to probe experimentally at the single molecule level. Computer simulations provide a unique view of membrane systems that complements experimental data, and have been used to study membrane phase behavior ²⁸. Coarsegrained simulations have been used extensively to study membrane domain formation ^{28–30}, including a recent simulation mimicking a real cell's plasma membrane ³¹. Atomistic simulations were only very recently shown to observe phase separation in a 10 microsecond simulation ³². Atomistic simulations of smaller model bilayers have shown many critical details regarding the properties of cholesterol containing bilayers. The condensing effect of cholesterol was shown in early simulations of 10's of nanoseconds ^{33,34}. There have been many atomistic simulations characterizing cholesterol interactions in lipid bilayers, with favorable packing between the flat face of cholesterol and saturated lipid tails ^{35,36}. Poly-unsaturated lipid tails have been shown to pack poorly with cholesterol ³⁷. Long time scale simulations with the all atom CHARMM36 force field have shown hexagonal packing of lipids in the l₀ phase, consistent with NMR measurements ³⁸. Free energies for lipid processes are difficult to calculate because of slow dynamics, strong electrostatic interaction for the head groups, water ordering and 'binding' at the interface, and collective interactions between neighboring lipids. Using umbrella sampling cholesterol has been shown to have a lower free energy in ordered bilayers ³⁹⁻⁴¹. We determined the free energy for removing a single DPPC lipid from bilayers with (up to 40 mol%) and without cholesterol 42. Contrary to conventional thinking, that cholesterol and a saturated lipid interact favorably, we found that DPPC had a lower free energy in the bilayer without cholesterol. This idea that cholesterol is "pushing" lipids, in addition to the attraction between cholesterol and the saturated lipid, has been suggested using nearest-neighbor recognition measurements 43. What is cholesterol's role in lipid bilayer phase behavior?

We have addressed the thermodynamics for the mixing of saturated and unsaturated PC lipids with cholesterol using atomistic computer simulations. Atomistic molecular dynamics simulations were used to observe domain formation during a 10 μs simulation from a random mixture. We used thermodynamic integration (TI) calculations to determine the free energy for exchanging an unsaturated and saturated lipid between the l_d and l_o phases. The free energy transformation was designed to get accurate statistics, by applying a minimal chemical change to the system, i.e. changing four double bonds to single bonds. The free energy for changing a DLiPC to a DSPC lipid in any l_d bilayer is favorable by $\sim\!20$ kJ/mol, irrespective of the composition or temperature, even in a DLiPC bilayer with 40 mol% cholesterol. In a gel phase, the free energy is more favorable ($\sim\!45$ kJ/mol), with enthalpically favorable packing of the lipids. In the l_o phase, we find a free energy of $\sim\!35\text{-}40$

kJ/mol, which is strongly temperature and concentration dependent and has a large unfavorable entropy change. Martini coarse-grained simulations show that the total free energy of lipid exchange is similar to the atomistic value, but the contributions are different. Neglecting lipid chain entropy is a necessary part of coarse-graining, and may be a relevant choice for a great number of problems, but limits the thermodynamic resolution of Martini and models of similar detail. We discuss the implications of our results on membrane phase behavior and cell biology.

Methods

AA simulations

Simulations were conducted using GROMACS version 4.5 ⁴⁴. The v-rescale method was used to maintain the temperature with a coupling constant of 0.1 ps ⁴⁵. Semi-isotropic pressure coupling with the Berendsen weak coupling method ⁴⁶, a compressibility of 4.5x10⁻⁵ bar⁻¹, a coupling constant of 2.5 ps, and a 1 bar reference pressure was used. The reaction-field method ⁴⁷ was used for long-range interactions after a 1.4 nm cut-off, with 62 for the dielectric constant of bulk water. A 7 fs time step was used by adding an additional bond from the hydrogen on the hydroxyl of cholesterol to the carbon adjacent to the oxygen, thus constraining the fast angle bending of the light hydrogen. Additionally, the mass of the water hydrogen's was set to 4 amu, at the expense of the oxygen (reduced to 12 amu) as suggested in ⁴⁸. The LINCS algorithm ⁴⁹ was used to constrain bonds and angles, and SETTLE for water ⁵⁰. The Berger lipid parameters were used for DSPC and DLiPC ⁵¹, with the double bond dihedrals from ⁵². The cholesterol model was based on the GROMOS force field ⁵³. The SPC water model was used ⁵⁴.

We tested the effect of the 7 fs time step and reaction field long-range electrostatics on the thermodynamics of lipid mixing by conducting TI calculations with PME for electrostatics and a 2 fs time step. The free energies are within the statistical error, and because we are concerned with thermodynamic properties this should not be a problem. The kinetic properties, particularly for the heavy water, would be influenced somewhat by the longer time step and shifted mass ⁴⁸.

Martini simulations

GROMACS 4.5 ⁴⁴ was used to run Martini 2.0 lipid coarse-grained simulations ⁵⁵. We used a 20 fs time step for the simulations. Electrostatic interactions were truncated at 1.2 nm and were treated with a switch-function from 0 to 1.2 nm. A dielectric constant of 15 is used for the electrostatic interactions. Lennard-Jones interactions were cut-off at 1.2 nm and a switch function was used between 0.9 and 1.2 nm. The Berendsen thermostat and

barostat were used with coupling constants of 0.4 and 1.1 ps, and a compressibility of 6.5×10^{-5} for the semi-isotropic pressure coupling 46 .

Systems

A large ca. 16 x 16 nm box with 352:352:320, DLiPC:DSPC:CHOL, lipids was first built with the Martini model. The system was equilibrated at 350 K to create a homogeneously mixed membrane. This structure was converted back to atomistic detail using the method in 56 . This large bilayer was simulated for 10 μ s with atomistic parameters as described above.

Using the Martini CG model we ran a 5 μ s simulation of a rectangular bilayer system with a 168:252:180 DLiPC:DSPC:CHOL ratio of lipids and observed phase separation into l_0 and l_d . Due to periodic boundary conditions we have infinitely long stripes of each phase. The system phase separated into a l_0 and l_d phase as expected from previous simulations 57 . We then converted the CG simulations to atomistic representation 56 and the simulation was continued with atomistic parameters.

Thermodynamic Integration

We ran thermodynamic integration calculations to determine the free energy for changing a saturated DSPC into a poly-unsaturated DLiPC. Both lipids have 18-carbon tails, so the same number of particles in the united atom Berger force field. For the conversion, we change 4 single bonds into 4 cis-double bonds, changing the bond lengths, angles, dihedrals, and the Lennard-Jones parameters. Because the Berger model is united atom, we do not have to change the number of atoms, simply changing the CH2 atom types to CH. This was accomplished in two steps: the force constant for the improper dihedral (which keeps the double bonds planar) was first reduced from 100 to 15. For this transformation we used 11 evenly spaced lambda windows and each simulation was 140 ns. The rest of the parameters including removing the improper dihedral, changing the Lennard-Jones parameters, and the bond angles were alchemically changed from DLiPC parameters to DSPC parameters in a second calculation. We note that for this transformation state A (DLiPC) had the reduced improper force constant of 15. As mentioned above, a second set of thermodynamic integration calculations that reduce the improper force constant from 15 to 0 was also calculated. For this transformation, we used 18 lambda values and 140 ns for each simulation. Changing all the parameters in one step led to instabilities at high lambda values due to the harmonic improper term. By adding together both free energies we obtain the total free energy for mutating DLiPC to DSPC. Error was estimated using the block averaging procedure ⁵⁸ for each umbrella window.

For the Martini model, we determined the free energy for converting a saturated 4-bead DSPC molecule into a 4-bead DLiPC. Due to the 4-to-1 mapping in Martini, lipid tails

represent a range of atomistic carbons, and we note that the 4-bead saturated tail is normally referred to as DPPC. A comparison of 5-bead lipids could be of future interest. For the thermodynamic integration calculation for the Martini DLiPC to DSPC transformation, the central tail beads Van der Waal's parameters and the bond angles are the only modified parameters.

Centered difference – entropy/enthalpy decomposition

From the basic definition of entropy (Eq. 1), the difference in entropy between two states can be estimated from the free energy difference at two different temperatures (Eq. 2).

$$S = -\left(\frac{\partial F}{\partial T}\right)_{N,P} (1)$$

$$\Delta S_{B-A} = -\frac{\Delta F_{B-A}^{TI}(T + \Delta T) - \Delta F_{B-A}^{TI}(T - \Delta T)}{2\Delta T} (2)$$

The difference in enthalpy can then be calculated using the difference in free energy and entropy (i.e. from $\Delta G = \Delta H - T\Delta S$).

Results

Atomistic domain formation

Starting from a random lateral distribution of cholesterol, DLiPC, and DSPC, we ran a 10 µs simulation and directly observed demixing of the bilayer (Fig. 1). At the start, we observe a more homogenous distribution in the lateral composition. The number of DSPC-DSPC contacts increases, the DLiPC-DSPC contacts decrease and the number of DSPC-cholesterol contacts increases marginally. This indicates phase separation, with preferential DSPC-DSPC interactions. Due to the small box size we do not expect full phase separation to occur – with most lipids near an interface between the ordered and disordered domains. The total potential energy of the entire system decreases as the domain forms (Fig. 1). The drop in energy is due to more favorable Lennard-Jones interactions and bonded interactions, while the short ranged electrostatic energy remains relatively constant despite large fluctuations. These results show that atomistically these lipids will undergo phase separation, but much larger simulations and longer time scales would be needed to observe bulk phase separation.

Martini lipid free energies

By determining the free energy to convert one lipid to another in both phases we can determine the relative concentration of each phase, or the excess chemical potential. At

equilibrium the chemical potential for each type of lipid must be equal in all phases of the system:

$$\mu_{DSPC, ORD}^{\circ} + RT \ln X_{DSPC,ORD} = \mu_{DSPC, DIS}^{\circ} + RT \ln X_{DSPC,DIS}$$
(3)
$$\mu_{DSPC} = \mu_{DSPC}^{\circ} + RT \ln X_{DSPC}$$
(4)
$$\Delta \mu_{DSPC, ORD-DIS}^{\circ} = RT \ln \frac{X_{DSPC,ORD}}{X_{DSPC,DIS}}$$
(5)
$$\Delta \Delta G_{exchange} = \Delta \mu_{DLPC-DSPC,ORD}^{\circ} - \Delta \mu_{DLPC-DSPC,DIS}^{\circ} = \Delta \mu_{DSPC,ORD-DIS}^{\circ} - \Delta \mu_{DLPC,ORD-DIS}^{\circ}$$
(6)

By calculating the free energy for exchange we can equate it to the excess chemical potential difference of DSPC and DLiPC in the two phases. In plain terms, we calculate the free energy for exchanging a single lipid between 2 phases, which we can use to determine the concentration difference of the 2 lipids in either phase. Figure 2 illustrates the connection between the chemical potential difference and concentration using the Martini model. We first ran a 5 μs simulation and observed domain formation in a long rectangular box, which creates a phase separated stripe because of periodic boundary conditions. From the number density of each lipid in the l_d and l_o phase, we determined $\Delta\Delta G_{exchange}$ to be 16.7 kJ/mol. We then restrained a single lipid in each phase and used TI to determine ΔG_{un-sat} , which we then used to determine a $\Delta\Delta G_{exchange}$ of 14.3 kJ/mol. The agreement between these two methods for calculating $\Delta\Delta G_{exchange}$ shows that TI can be used to study lipid mixing, with the benefit of reduced sampling.

We determined $\Delta G_{un\text{-sat}}$ for small lipid systems with the Martini model. First, we built small bilayers for the l_d and l_o phases based on the lipid densities in the stripe domain system, 84:4:12 and 2:59:39 ratios of DLiPC:DSPC:CHOL, respectively. Table 1 shows that these systems have very similar values for $\Delta G_{un\text{-sat}}$ as the stripe bilayer, 6.1 kJ/mol (l_d) and 9.6 kJ/mol (l_o). Combing these two numbers using eq. 6, gives $\Delta \Delta G_{exchange}$ of 15.7 kJ/mol, which is in better agreement with $\Delta \Delta G_{exchange}$ from the lipid densities, likely because of better sampling, and possible artifacts from restraining the lipid in the stripe phase. $\Delta G_{un\text{-sat}}$ values were also calculated for one and two-component mixtures (Table 1). In the disordered pure DLiPC bilayer $\Delta G_{un\text{-sat}}$ was 9.5 kJ/mol, and -3.2 kJ/mol in the pure DSPC bilayer. A higher $\Delta G_{un\text{-sat}}$ of -13.8 kJ/mol was calculated in a DSPC-40mol% cholesterol mixture, because this system is more ordered that the l_o system.

An improved Martini cholesterol model was recently shown to reduce the solid nature of l_0 bilayers, in better agreement with experiments and simulations 31 . We tested the effect of the old Martini compared to Martini v2.2 cholesterol in a DSPC-40mol% cholesterol bilayer (Table 1). As expected the newer cholesterol resulted in a lower $\Delta G_{un\text{-sat}}$

(-13.8 kJ/mol compared to -21.4 kJ/mol), because the bilayer is less ordered. The stripe domain bilayers $\Delta G_{un\text{-sat}}$ showed this same trend (Table 1).

Atomistic lipid free energies

Based on the Martini simulations, we are confident that we can use TI calculations to determine the free energy of lipid mixing. We determined the free energy to alchemically convert DLiPC to DSPC in a number of atomistic membrane systems using thermodynamic integration. Fig. 3 shows the systems studied: pure DLiPC and DSPC (at 335 K) l_d bilayers, a 3:2 DSPC:CHOL mixture in the l_0 phase, and a gel DSPC bilayer. In all membrane environments, we find a favorable free energy for converting DLiPC to DSPC. Table 2 lists the free energy in various membranes at a number of different temperatures and phases. The free energy is favorable for changing DLiPC to DSPC, in all cases, and very favorable for the gel DSPC and the l_0 phase. We found $\Delta G_{un\text{-sat}}$ is ca. -20 kJ/mol in the l_d phase, both in the DLiPC bilayer at 300 K and in the DSPC bilayer at 335 K, and the DLiPC bilayer with 40% cholesterol. We find the lowest free energy of -45 kJ/mol in the DSPC bilayer at 300 K, which is in the gel state. In the l_0 phases, we find intermediate values for the free energy that are dependent on the amount of cholesterol and the temperature of the system.

Using the thermodynamic cycle in Fig. 4, we determined $\Delta\Delta G_{exchange}$ for exchanging DLiPC and DSPC between l_d and l_o phases in a stipe domain. The agreement with the Martini model is within the error, with $\Delta\Delta G_{exchange}$ of 14 kJ/mol for both atomistic and for Martini. We note that these domains may not reflect the equilibrium lipid composition, as they were constructed from Martini phase separated systems. But the fact that we find very similar $\Delta G_{un\text{-}sat}$ for the different phases as for the small bilayer patches shows that qualitatively the agreement is still good (Table 2). For the l_d domain, we find a free energy of -21 kJ/mol, in close agreement with all other liquid phase systems. The free energy of -35 kJ/mol for the l_o phase is close to the -39 kJ/mol for the small 40% cholesterol system. The discrepancy is likely due to the different lipid compositions between the small system and the l_o stripe phase, which likely had less cholesterol and some DLiPC. Overall $\Delta\Delta G_{exchange}$ is unfavorable by 14 kJ/mol, which is expected given that they phase separate (Fig. 3). It is important to note that while the agreement between Martini and atomistic systems for $\Delta\Delta G_{exchange}$ is good, the contributions are completely opposite.

Entropy and lipid conformational freedom

By determining the free energy of exchange at different temperatures we can estimate the change in entropy for $\Delta\Delta G_{exchange}$ using the centered difference method (see Methods). In the l_d phase, we find a near zero change in entropy, compared to an unfavorable change of –T ΔS of ca. 156 kJ/mol in the l_o phase (Table 3). We note that this is the entropy change for the entire system, not just the configurational entropy of the perturbed lipid. In the l_o bilayer, the exchange results in a favorable enthalpy of -194

kJ/mol. The packing of saturated lipids in the l_0 phase results in large favorable enthalpy changes, but is opposed by an unfavorable entropy change. This matches our expections from the reduced potential energy in the large system that phase separates (Fig. 1).

We aligned the molecular conformations of a single DLiPC and DSPC in the l_{o} and l_{d} phases (Fig. 5). Both lipids adapt to the local environment of the bilayer; with restricted conformations in the l_{o} domain and more varied molecular conformations in the l_{d} phase. In the l_{d} phase, we find that both DLiPC and DSPC sample a large distribution of different conformations, although the distribution for DLiPC is noticeably broader than DSPC. While not quatitative these figures strongly suggest that the large entropic contribution is not solely from changes in configurational entropy of the single exchanging lipid.

Discussion

Cholesterol induced domain formation

We have used molecular dynamics simulations to explore the atomic level details for cholesterol mixed with saturated and poly-unsaturated phospholipids. Novel free energy calcalations are used to determine the thermodynamic basis for phospholipid partitioning between l_d and l_o phases. In general, our results support the traditional view of the ordering effect of cholesterol on saturated phospholipids. This behavior is often explained to be due to the chemical structure of cholesterol, with a small head group, and rigid sterol body, that interacts favorably with saturated lipid tails. Our results show that a major driving force for domain formation is due to the unfavorable entropy of a poly-unsaturated phospholipid residing in the ordered domain.

The Martini model has been used extensively to study membrane domain formation ^{57,59} due to the slow dynamics and computational cost of atomistic simulations ⁶⁰. We observed the start of domain formation in a ternary lipid mixture of cholesterol, DLiPC, and DSPC, using atomistic molecular dynamics computer simulations. The system is too small (15 nm x 15 nm bilayer) to observe true phase separation, where interfacial interactions would dominate over bulk behavior of the lipids in our small bilayer patch. This result shows that the Berger lipid parameters can qualitatively reproduce the experimental phase diagrams of model membranes with cholesterol, saturated and unsaturated ^{15,61}. This is in agreement with a previous study comparing Berger and Martini parameters for equilibrium domain formation in a cholesterol:DLiPC:DPPC mixture ³². In-depth analysis showed that Martini can reproduce the general structural mechanism for domain formation, but is 40 times faster than atomistic ³². Many other previous atomistic simulations have shown preferential interactions of cholesterol with saturated lipids ^{33,34}. From our energy decompositions (Fig. 1), we show that domain formation is enthalpically favorable, due to

more trans bond conformations and Van der Waals interactions when cholesterol interacts with the saturated lipid tails. But the enthalpic gain is offset by a large and unfavorable entropic contribution, which we determined with free energy calculations.

Free energy calculations can address the underlying driving forces for domain formation. We use the Martini model to show that our free energy calculations are directly related to the difference in concentration for each lipid in either phase. The advantage of using free energy calculations is that we can use smaller bilayers and obtain adequate statistics because of the small perturbation of changing 4 double bonds to single bonds. The most favorable environment for the transformation of DLiPC to DSPC is in the gel-DSPC phase followed by the l₀ phase. There is a trend that more cholesterol makes the transformation more favorable: there was more local cholesterol in the 3:2 DSPC:CHOL bilayer than in the l_0 phase in the stripe domain system, and a lower ΔG_{un-sat} in the 3:2 system. The favorable free energy of the saturated lipid is due to the formation of stronger enthalpic interactions, at the expense of considerable entropy. In all the l_d bilayers we studied, we found very similar values for the ΔG_{un-sat} , due to slightly more favorable enthalpic interactions for the saturated lipid. In the l_d phase, there is a near zero change in entropy for changing the unsaturated to saturated lipid because the disordered liquid state does not restrict lipid tail conformations. Interestingly, 40 mol% cholesterol mixed with DLiPC results in a l_d phase bilayer, indicating that poly-unsaturated lipids cannot pack into an l₀ phase.

We could directly compare our $\Delta\Delta G_{exchange}$ values to the concentration differences in the two phases determined from the tie lines of experimental phase diagrams. Quantitative comparison is not possible because we are unaware of a DSPC:DLiPC:Cholesterol phase diagram, and the tie lines from experimental diagrams are difficult to obtain accurately 62 . Qualitatively our results match experimental studies predicting enrichment of the saturated phospholipid in the l_0 phase and the unsaturated lipid in the l_d phase.

Models: when do chemical details matter?

The Martini model has been used extensively to study lipid bilayer domains 28 . By determining thermodynamic parameters for the process of lipid mixing we are able to address the molecular driving forces. We find that while Martini does semi-quantitatively match the atomistic $\Delta\Delta G_{\text{exchange}}$ the underlying components are different. For the atomistic model, we find that converting the unsaturated lipid to saturated in the l_d phase is favorable, while for Martini this is unfavorable. This is most likely due to the reduced representation in the Martini model, where a large portion of the lipid's entropy has been replaced by enthalpic interactions. This was previously noted in the first version of the Martini model 63 . Whether either model is correct remains to be settled with experimental evidence, but the difference is striking.

The success of Martini in modeling lipid phase behavior ^{28,30,57}, and other models of similar detail 64 suggests that some degrees of freedom can be neglected and observe many interesting phenomena. Even more simple continuum models, phenomenological models, and lattice models have reproduced many aspects of lipid mixing and added to our understanding of lipid phase behavior 65-69. But our results calls into question using Martini - and likely other CG models of similar and lower resolution - to obtain quantitative thermodynamic analysis for lipid mixing at the molecular level. One may obtain surprisingly accurate free energies of transfer, and the distribution of all the molecules in an entire plasma membrane patch 31, but the underlying molecular level physical mechanism and thermodynamics are not necessarily correct. This is not to deny the utility of such models, but to set boundaries on the types of problems that can be solved with a particular model. We show that the recently updated Martini cholesterol parameters improve the agreement with atomistic free energies for DLiPC-DSPC lipid exchange. This is due to the earlier cholesterol molecule forming a too rigid l₀ phase, noted in ³¹. Similar free energy calculations may prove useful for parameterizing and validating lipid models, especially if linked to experimental thermodynamic data in the future.

Biomembrane implications

Our results show that phase separation in simple model systems is a complex process, and illustrates the importance of phospholipid conformations and double bonds on the molecular level energetics. While the total free energy is relatively small, we find very high entropy and enthalpy contributions. Enthalpy-entropy compensation is a well-known phenomenon in many other biological problems, such as drug-binding and protein-protein interactions ⁷⁰. It has been suggested that the magnitude for the entropy is much too large to be attributed to conformation of the macromolecule, and therefore must include solvation contributions ⁷⁰. Based on our RMSD fit for DLiPC and DSPC shown in Fig. 5, we suggest that the conformational entropy change for the single exchanging lipid would be extremely small. We speculate that the large entropy change could be due to the 'solvation' of the exchanging lipid by the surrounding lipids in the bilayer.

The large enthalpic and entropic contributions could be a convenient way for the cell to control lipid localization – with a high fidelity switch between ordered-disordered. For example, being near a membrane protein, or cytoskeleton may shift this balance. The large entropic contribution means that subtle changes in temperature could also be used to 'activate' this lipid 'switch'. It will be interesting to run similar free energy calculations on membrane protein bound phospholipids. Most biologically relevant phospholipids have one saturated tail and one unsaturated tail, so investigating mono-unsaturated lipids using the same protocol would be of interest.

The phase behavior of simple lipid mixtures and the molecular level details for lipid mixing have many biological applications. The complexity of a real cell membrane - with actin cytoskeleton, membrane proteins, ion gradients and thousands of lipid types – makes simple model systems necessary to characterize the molecular details. Understanding the physicochemical properties of membranes at the molecular level will allow critical advances in personalized medicine, including drug delivery, membrane protein localization and function, new drugable sites on GPCRs, ion channels and multidrug transporters, and peptide aggregation, such as amyloid peptides, and cationic penetrating peptides. Methods similar to ours may help in many future investigations.

Conclusions

Phase separation in cholesterol, saturated and unsaturated phosphatidylcholine lipid bilayers is described with molecular level details. We show that lipid domain formation is caused by more favorable enthalpic interactions for the saturated lipid in the l_0 phase, despite a large unfavorable shift in entropy. Both saturated and unsaturated lipids have similar conformations in each phase and more favorable enthalpy. The reduced number of degrees of freedom of the Martini model's tails means the free energy for domain formation has little conformational entropy contribution. This suggests that while Martini can reproduce the general distribution of lipids in l_0 and l_d phases, the molecular driving forces are different than atomistic models. Important atomistic details for lipid mixing are presented with implications for cellular membrane domain formation.

Acknowledgements

This work was supported by the Natural Sciences and Engineering Research Council (NSERC). D.P.T. is an Alberta Innovates Technology Futures Strategic Chair in (Bio)Molecular Simulation. This work was undertaken, in part, thank to funding from the Canada Research Chairs program. J.-E.S. is supported by National Science Foundation MCB 1716956. W.F.D.B. was supported by fellowships from NSERC, the Canadian Institute for Health Research, and the NSERC Banting Fellowship. W.F.D.B. was also supported by National Science Foundation CHE 1465162. Simulations were run on Compute Canada facilities, supported by the Canada Foundation for Innovation. This work used the Extreme Science and Engineerging Discovery Environment, which is supported by National Science Foundation grant number ACI-1548562 (MCA05S027 and MCB160067).

Tables

Table 1: Martini $\Delta G_{un\text{-sat}}$ values

Bilayer	Temperature (K)	ΔG _{un-sat} (kJ/mol)
DLiPC	300	9.5 ± 0.1
DSPC	300	-3.2
DSPC- 40%CHOL	300	-21.4 ± 2.1
Stripe-L _d	300	7.3± 0.9
Stripe-L _o	300	-13.2± 3.1
DSPC- 40%CHOL - v2.2	300	-13.8
Small-L _d - v2.2	300	6.1
Small- $L_0 - v2.2$	300	-9.6
Stripe-L _d – v2.2	300	5.8
Stripe-L _o -v2.2	300	-8.5

Table 2: Atomistic $\Delta G_{DLiPC-DSPC}$ values

Bilayer (phase)	Temperature (K)	ΔG _{un-sat} (kJ/mol)
DLiPC	300	-20.2±1.0
DLiPC	310	-19.9±0.7
DLiPC	320	-20.3±0.6
DLiPC	335	-20.4±0.5
DLiPC-40%CHOL	300	-21.9±0.8
DSPC (liq.)	335	-21.4±0.8
DSPC (gel)	300	-44.6±3.2
DSPC- 40%CHOL	300	-39.9±1.3
DSPC-40%CHOL	310	-37.8±1.7
DSPC-40%CHOL	320	-29.8±1.9
Stripe-Ord	300	-35.3±2.6
Stripe-Dis	300	-21.0±2.2

Table 3: Entropy and enthalpy decomposition for unsaturated to saturated lipid alchemical transformations.

Bilayer (Temperature (K))	-TΔS (kJ/mol)	ΔH (kJ/mol)
DLiPC (317)	-1	-19 kJ/mol
DSPC-CHOL (310)	156	-194 kJ/mol

Figures

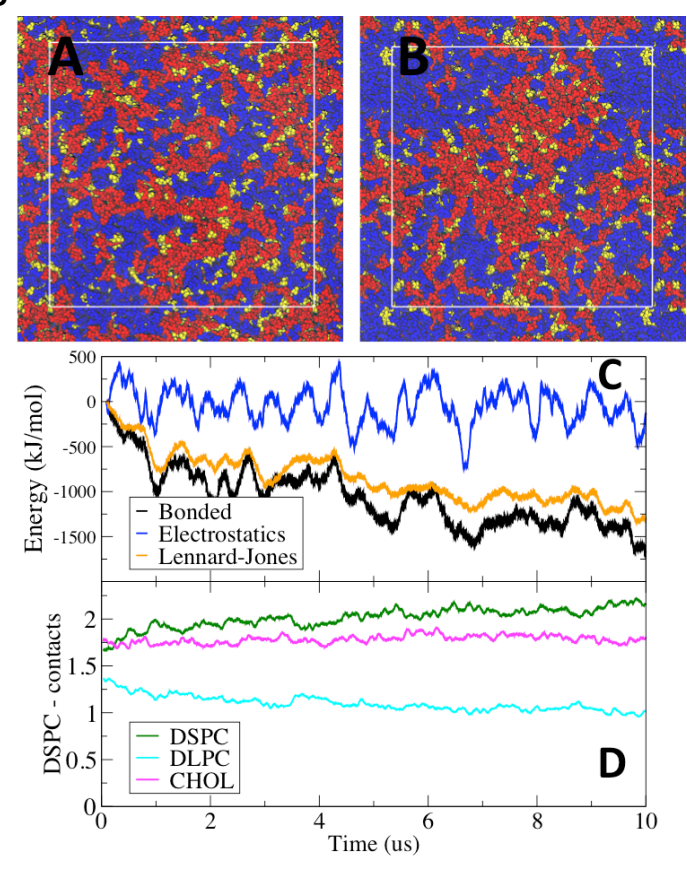


Figure 1: **A.** Top view of the large DSPC (red): DLiPC (blue): cholesterol (yellow) at the start of the simulation. The periodic box is shown as a white square. **B.** Snapshot after 10 μs of simulation, showing domain formation. **C.** Energetic contributions during bilayer phase separation in the large DSPC:DLiPC:cholesterol bilayer. Each component was set to 0 kJ/mol at the start of the simulation. **D.** The number of contacts between each type of lipid and DSPC during phase separation. A distance cut-off of 1.0 nm between the central carbon in the glycerol backbone for the PC lipids and the oxygen of cholesterol was used.

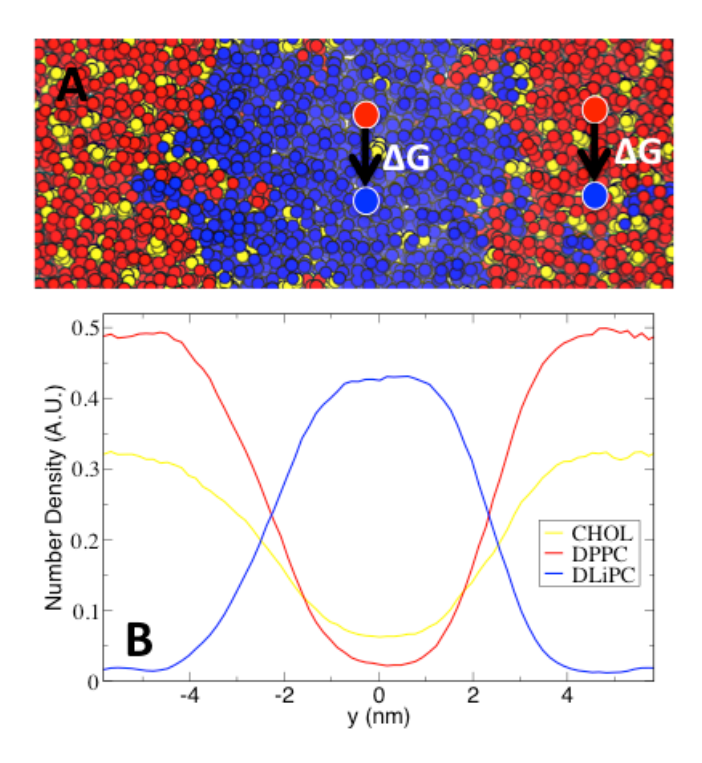


Figure 2: Calculating ΔG_{ex} using lipid densities and TI calculations with the Martini model. **A.** Phase separated bilayer of DSPC (red), DLPC (blue) and cholesterol (yellow), looking down on the top of the bilayer. The blue rectangle shows the unit cell of the simulation. **B.** Average lipid densities across the bilayer, calcuted after the bilayer phase separated.

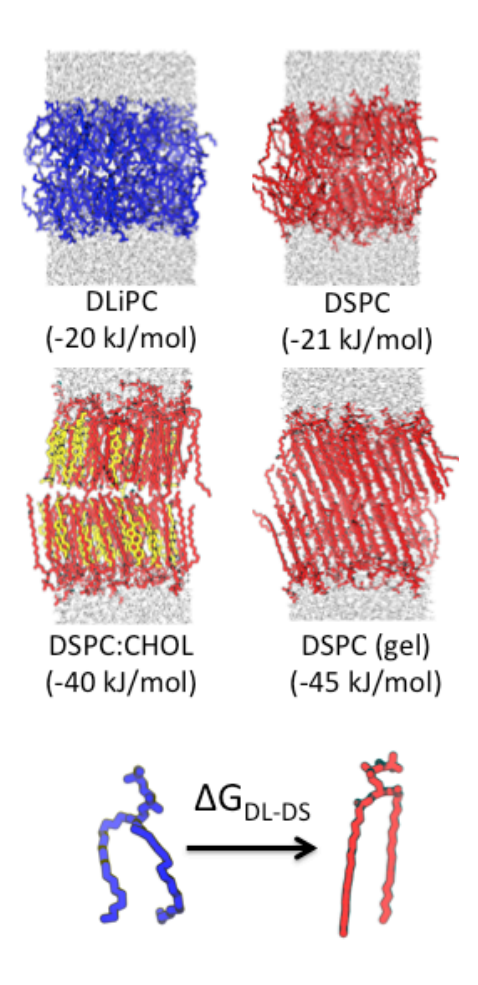


Figure 3: Atomistic free energies for the alchemical transformation of DLiPC to DSPC in different membrane environments. Colors are the same as Fig. 2, with water colored white.

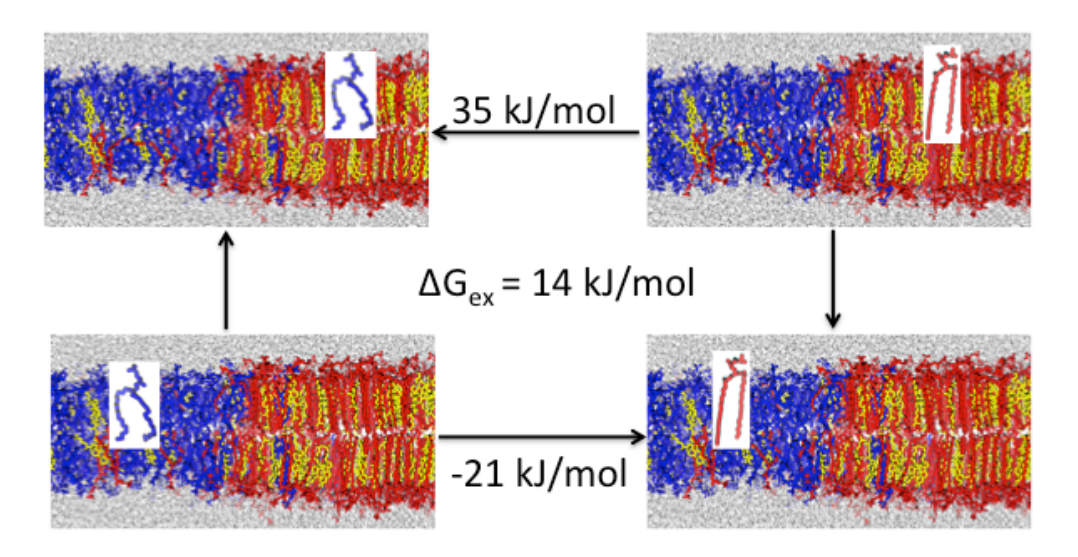


Figure 4: Thermodynamic cycle for exchanging a single DSPC in the l_o phase for a DLiPC in the l_d phase. Adding these two components gives the total free energy for exchange $(\Delta\Delta G_{exchange})$.

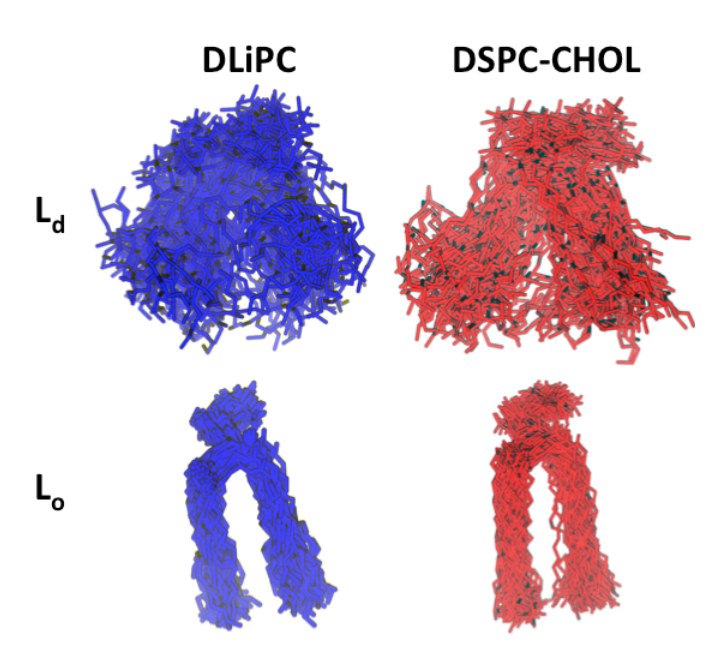


Figure 5: Single lipid conformations in the different domains of the stripe bilayer. Each structure was aligned using a RMSD fit.

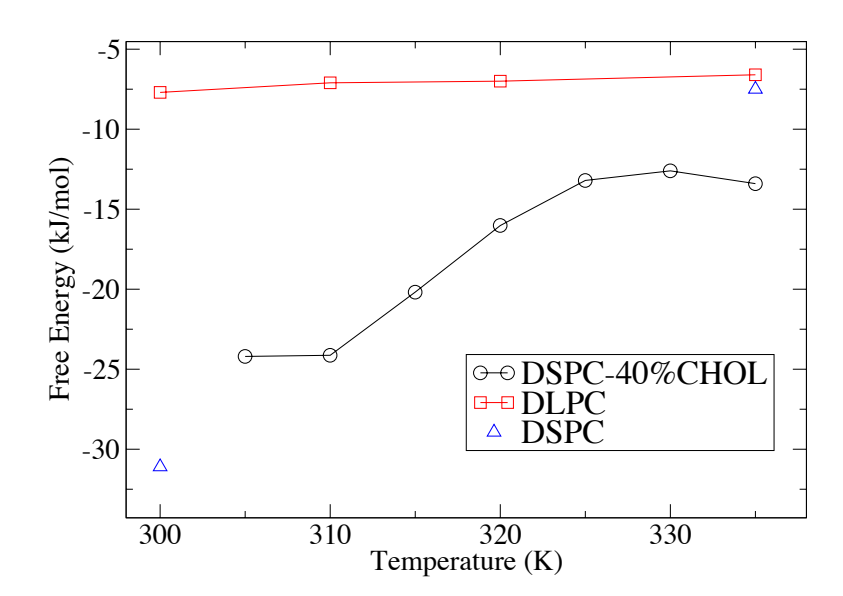


Figure 6: Temperature dependence of $\Delta G_{\text{un-sat}}$ for the different atomistic bilayers.

I am not sure about including this, although I have a huge amount of new temp. calculations for Martini too.

References

- 1. Simons, K. & Ikonen, E. Functional rafts in cell membranes. *Nature* **387**, 569–572 (1997).
- 2. Stier, A. & Sackmann, E. Spin labels as enzyme substrates Heterogeneous lipid distribution in liver microsomal membranes. *Biochim. Biophys. Acta (BBA)-Biomembranes* **311**, 400–408 (1973).
- 3. Lingwood, D. & Simons, K. Lipid rafts as a membrane-organizing principle. *Science* **327**, 46–50 (2010).
- 4. Eggeling, C. *et al.* Direct observation of the nanoscale dynamics of membrane lipids in a living cell. *Nature* **457**, 1159–1162 (2009).
- 5. Mueller, V. *et al.* STED Nanoscopy Reveals Molecular Details of Cholesterol- and Cytoskeleton-Modulated Lipid Interactions in Living Cells. *Biophys. J.* **101**, 1651–1660 (2011).
- 6. Boxer, S. G., Kraft, M. L. & Weber, P. K. Advances in imaging secondary ion mass spectrometry for biological samples. *Annu. Rev. Biophys.* **38**, 53–74 (2009).
- 7. Frisz, J. F. *et al.* Direct chemical evidence for sphingolipid domains in the plasma membranes of fibroblasts. *Proc. Natl. Acad. Sci.* **110**, E613–E622 (2013).
- 8. Frisz, J. F. *et al.* Sphingolipid domains in the plasma membranes of fibroblasts are not enriched with cholesterol. *J. Biol. Chem.* **288**, 16855–16861 (2013).
- 9. Kraft, M. L. *et al.* High-Resolution Imaging of the Distributions of Cholesterol, Sphingolipids, and Specific Proteins in the Plasma Membrane with Secondary Ion Mass Spectrometry. *Microsc. Microanal.* **21**, 2397–2398 (2015).
- 10. van Meer, G., Voelker, D. R. & Feigenson, G. W. Membrane lipids: where they are and how they behave. *Nat. Rev. Mol. Cell Biol.* **9,** 112–124 (2008).
- 11. Viola, A. & Gupta, N. Tether and trap: regulation of membrane-raft dynamics by actin-binding proteins. *Nat. Rev. Immunol.* **7**, 889–896 (2007).
- 12. Elson, E. L., Fried, E., Dolbow, J. E. & Genin, G. M. Phase separation in biological membranes: integration of theory and experiment. *Annu. Rev. Biophys.* **39**, 207 (2010).
- 13. Fan, J., Sammalkorpi, M. & Haataja, M. Formation and regulation of lipid microdomains in cell membranes: theory, modeling, and speculation. *FEBS Lett.* **584**, 1678–1684 (2010).
- 14. McConnell, H. M., Tamm, L. K. & Weis, R. M. Periodic structures in lipid monolayer phase transitions. *Proc. Natl. Acad. Sci.* **81**, 3249–3253 (1984).
- 15. Feigenson, G. W. Phase diagrams and lipid domains in multicomponent lipid bilayer mixtures. *Biochim. Biophys. Acta (BBA)-Biomembranes* **1788,** 47–52 (2009).
- 16. Heftberger, P., Kollmitzer, B., Rieder, A. A., Amenitsch, H. & Pabst, G. In situ determination of structure and fluctuations of coexisting fluid membrane domains. *Biophys. J.* **108**, 854–862 (2015).

- 17. Konyakhina, T. M. *et al.* Control of a nanoscopic-to-macroscopic transition: modulated phases in four-component DSPC/DOPC/POPC/Chol giant unilamellar vesicles. *Biophys. J.* **101**, L8–L10 (2011).
- 18. Heberle, F. A., Wu, J., Goh, S. L., Petruzielo, R. S. & Feigenson, G. W. Comparison of three ternary lipid bilayer mixtures: FRET and ESR reveal nanodomains. *Biophys. J.* **99**, 3309–3318 (2010).
- 19. Ackerman, D. G. & Feigenson, G. W. Multiscale modeling of four-component lipid mixtures: domain composition, size, alignment, and properties of the phase interface. *J. Phys. Chem. B* **119**, 4240–4250 (2015).
- 20. Ackerman, D. G. & Feigenson, G. W. Lipid bilayers: clusters, domains and phases. *Essays Biochem.* **57**, 33–42 (2015).
- 21. Feigenson, G. W. Phase boundaries and biological membranes. *Annu. Rev. Biophys. Biomol. Struct.* **36**, 63 (2007).
- 22. Hsueh, Y., Zuckermann, M. & Thewalt, J. Phase diagram determination for phospholipid/sterol membranes using deuterium NMR. *Concepts Magn. Reson. Part A* **26**, 35–46 (2005).
- 23. Engberg, O. *et al.* Lipid Interactions and Organization in Complex Bilayer Membranes. *Biophys. J.* **110**, 1563–1573 (2016).
- 24. Khadka, N. K., Ho, C. S. & Pan, J. Macroscopic and Nanoscopic Heterogeneous Structures in a Three-Component Lipid Bilayer Mixtures Determined by Atomic Force Microscopy. *Langmuir* **31**, 12417–12425 (2015).
- 25. Yasuda, T., Tsuchikawa, H., Murata, M. & Matsumori, N. Deuterium NMR of raft model membranes reveals domain-specific order profiles and compositional distribution. *Biophys. J.* **108**, 2502–2506 (2015).
- 26. Giang, H., Shlomovitz, R. & Schick, M. Microemulsions, modulated phases and macroscopic phase separation: a unified picture of rafts. *Essays Biochem.* **57,** 21–32 (2015).
- 27. Sezgin, E. *et al.* Partitioning, diffusion, and ligand binding of raft lipid analogs in model and cellular plasma membranes. *Biochim. Biophys. Acta Biomembr.* **1818**, 1777–1784 (2012).
- 28. Bennett, W. F. D. & Tieleman, D. P. Computer simulations of lipid membrane domains. *Biochim. Biophys. Acta Biomembr.* (2013). doi:http://dx.doi.org/10.1016/j.bbamem.2013.03.004
- 29. Baoukina, S., Monticelli, L., Risselada, H. J., Marrink, S. J. & Tieleman, D. P. The molecular mechanism of lipid monolayer collapse. *Proc. Natl. Acad. Sci. U. S. A.* **105**, 10803–10808 (2008).
- 30. Marrink, S. J. & Tieleman, D. P. Perspective on the Martini model. *Chem. Soc. Rev.* **42**, 6801–22 (2013).
- 31. Ingólfsson, H. I. *et al.* Lipid Organization of the Plasma Membrane. *J. Am. Chem. Soc.* **136**, 14554–14559 (2014).

- 32. Hakobyan, D. & Heuer, A. Phase Separation in a Lipid/Cholesterol System: Comparison of Coarse-Grained and United-Atom Simulations. *J. Phys. Chem. B* **117**, 3841–3851 (2013).
- 33. Róg, T., Pasenkiewicz-Gierula, M., Vattulainen, I. & Karttunen, M. Ordering effects of cholesterol and its analogues. *Biochim. Biophys. Acta (BBA)-Biomembranes* **1788**, 97–121 (2009).
- 34. Berkowitz, M. L. Detailed molecular dynamics simulations of model biological membranes containing cholesterol. *Biochim. Biophys. Acta (BBA)-Biomembranes* **1788**, 86–96 (2009).
- 35. Róg, T., Pasenkiewicz-Gierula, M., Vattulainen, I. & Karttunen, M. What happens if cholesterol is made smoother: importance of methyl substituents in cholesterol ring structure on phosphatidylcholine–sterol interaction. *Biophys. J.* **92**, 3346–3357 (2007).
- 36. Martinez-Seara, H., Róg, T., Karttunen, M., Vattulainen, I. & Reigada, R. Cholesterol induces specific spatial and orientational order in cholesterol/phospholipid membranes. *PLoS One* **5**, e11162 (2010).
- 37. Pitman, M. C., Suits, F., MacKerell, A. D. & Feller, S. E. Molecular-level organization of saturated and polyunsaturated fatty acids in a phosphatidylcholine bilayer containing cholesterol. *Biochemistry* **43**, 15318–15328 (2004).
- 38. Sodt, A. J., Sandar, M. L., Gawrisch, K., Pastor, R. W. & Lyman, E. The Molecular Structure of the Liquid-Ordered Phase of Lipid Bilayers. *J. Am. Chem. Soc.* **136**, 725–732 (2014).
- 39. Bennett, W. F. D., MacCallum, J. L., Hinner, M. J., Marrink, S. J. & Tieleman, D. P. Molecular View of Cholesterol Flip-Flop and Chemical Potential in Different Membrane Environments. *J. Am. Chem. Soc.* **131**, 12714–12720 (2009).
- 40. Zhang, Z., Lu, L. & Berkowitz, M. L. Energetics of cholesterol transfer between lipid bilayers. *J. Phys. Chem. B* **112**, 3807–3811 (2008).
- 41. Bennett, W. F. D. & Tieleman, D. P. Molecular simulation of rapid translocation of cholesterol, diacylglycerol, and ceramide in model raft and nonraft membranes. *J. Lipid Res.* **53**, 421–429 (2012).
- 42. Bennett, W. F. D., MacCallum, J. L. & Tieleman, D. P. Thermodynamic analysis of the effect of cholesterol on dipalmitoylphosphatidylcholine lipid membranes. *J. Am. Chem. Soc.* **131**, 1972–1978 (2009).
- 43. Wang, C., Krause, M. R. & Regen, S. L. Push and Pull Forces in Lipid Raft Formation: The Push Can Be As Important As the Pull. *J. Am. Chem. Soc.* **137**, 150101223737006 (2015).
- 44. Hess, B., Kutzner, C., van der Spoel, D. & Lindahl, E. GROMACS 4: Algorithms for Highly Efficient, Load-Balanced, and Scalable Molecular Simulation. *J. Chem. Theory Comput.* **4,** 435–447 (2008).
- 45. Bussi, G., Donadio, D. & Parrinello, M. Canonical sampling through velocity rescaling. *J. Chem. Phys.* **126**, 014101 (2007).

- 46. Berendsen, H. J. C., Postma, J. P. M., van Gunsteren, W. F., DiNola, A. & Haak, J. R. Molecular dynamics with coupling to an external bath. *J. Chem. Phys.* **81**, 3684–3690 (1984).
- 47. Tironi, I. G., Sperb, R., Smith, P. E. & van Gunsteren, W. F. A generalized reaction field method for molecular dynamics simulations. *J. Chem. Phys.* **102**, 5451–5459 (1995).
- 48. Feenstra, K. A., Hess, B. & Berendsen, H. J. C. Improving efficiency of large timescale molecular dynamics simulations of hydrogen-rich systems. *J Comput Chem* **20**, 786–798 (1999).
- 49. Hess, B., Bekker, H., Berendsen, H. J. C. & Fraaije, J. G. E. M. LINCS: a linear constraint solver for molecular simulations. *J. Comput. Chem.* **18**, 1463–1472 (1997).
- 50. Miyamoto, S. & Kollman, P. A. SETTLE: an analytical version of the SHAKE and RATTLE algorithm for rigid water models. *J. Comput. Chem.* **13**, 952–962 (1992).
- 51. Berger, O., Edholm, O. & Jähnig, F. Molecular dynamics simulations of a fluid bilayer of dipalmitoylphosphatidylcholine at full hydration, constant pressure, and constant temperature. *Biophys. J.* **72**, 2002 (1997).
- 52. Bachar, M., Brunelle, P., Tieleman, D. P. & Rauk, A. Molecular dynamics simulation of a polyunsaturated lipid bilayer susceptible to lipid peroxidation. *J. Phys. Chem. B* **108**, 7170–7179 (2004).
- 53. Höltje, M. *et al.* Molecular dynamics simulations of stratum corneum lipid models: fatty acids and cholesterol. *Biochim. Biophys. Acta (BBA)-Biomembranes* **1511,** 156–167 (2001).
- 54. Berendsen, H. J. C., Postma, J. P. M., Van Gunsteren, W. F. & Hermans, J. in *Intermol. forces* 331–342 (Springer Netherlands, 1981).
- 55. Marrink, S. J., Risselada, H. J., Yefimov, S., Tieleman, D. P. & de Vries, A. H. The MARTINI force field: Coarse grained model for biomolecular simulations. *J. Phys. Chem. B* **111**, 7812–7824 (2007).
- 56. Rzepiela, A. J. *et al.* Reconstruction of atomistic details from coarse-grained structures. *J. Comput. Chem.* **31,** 1333–1343 (2010).
- 57. Risselada, H. J. & Marrink, S. J. The molecular face of lipid rafts in model membranes. *Proc. Natl. Acad. Sci.* **105,** 17367–17372 (2008).
- 58. Hess, B. Determining the shear viscosity of model liquids from molecular dynamics simulations. *J. Chem. Phys.* **116**, 209–217 (2002).
- 59. Bennett, W. F. D. & Tieleman, D. P. Computer simulations of lipid membrane domains. *Biochim. Biophys. Acta* **1828**, 1765–76 (2013).
- 60. Hong, C., Tieleman, D. P. & Wang, Y. Microsecond molecular dynamics simulations of lipid mixing. *Langmuir* **30**, 11993–12001 (2014).
- 61. Veatch, S. L. & Keller, S. L. Seeing spots: complex phase behavior in simple membranes. *Biochim. Biophys. Acta (BBA)-Molecular Cell Res.* **1746,** 172–185 (2005).
- 62. Uppamoochikkal, P., Tristram-Nagle, S. & Nagle, J. F. Orientation of Tie-Lines in the Phase Diagram of DOPC/DPPC/Cholesterol Model Biomembranes. *Langmuir* **26**,

- 17363-17368 (2010).
- 63. Baron, R. *et al.* Comparison of Thermodynamic Properties of Coarse-Grained and Atomic-Level Simulation Models. *ChemPhysChem* **8**, 452–461 (2007).
- 64. de Meyer, F. & Smit, B. Effect of cholesterol on the structure of a phospholipid bilayer. *Proc. Natl. Acad. Sci.* **106**, 3654–3658 (2009).
- 65. Brown, F. L. H. Continuum simulations of biomembrane dynamics and the importance of hydrodynamic effects. *Q. Rev. Biophys.* **44,** 391–432 (2011).
- 66. Brewster, R., Pincus, P. A. & Safran, S. A. Hybrid lipids as a biological surface-active component. *Biophys. J.* **97**, 1087–1094 (2009).
- 67. Bagatolli, L. & Kumar, P. B. S. Phase behavior of multicomponent membranes: Experimental and computational techniques. *Soft Matter* **5**, 3234–3248 (2009).
- 68. Huang, J. & Feigenson, G. W. A microscopic interaction model of maximum solubility of cholesterol in lipid bilayers. *Biophys. J.* **76**, 2142–2157 (1999).
- 69. Elliott, R., Szleifer, I. & Schick, M. Phase diagram of a ternary mixture of cholesterol and saturated and unsaturated lipids calculated from a microscopic model. *Phys. Rev. Lett.* **96**, 98101 (2006).
- 70. Dragan, A. I., Read, C. M. & Crane-Robinson, C. Enthalpy-entropy compensation: the role of solvation. *Eur. Biophys. J.* **46**, 301–308 (2017).

Supplementary Information

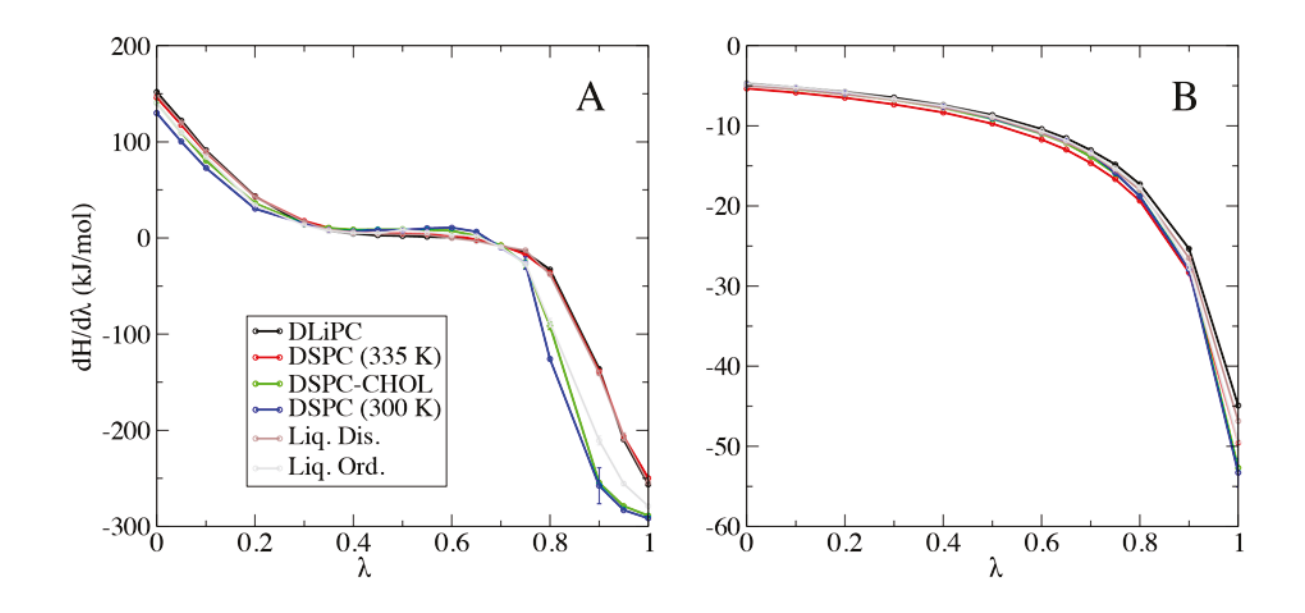


Figure S1: A. $dH/d\lambda$ curves for changing the bond lengths, angles, dihedrals and atom types from DLiPC to DSPC. B. $dH/d\lambda$ for reducing the force constant of the improper dihedrals in the double bonds of DLiPC.